Indian Journal of Pure & Applied Physics
Vol. 56, June 2018, pp. 423-427

LPG sensing application of *ex situ* PPy-Bi_2O_3-MOX (MOX=ZrO_2, Ag_2O and TiO_2) nanocomposites

A R Choudhary[a] & S A Waghuley[b]*

[a]Department of Physics, Suresh Deshmukh College of Engineering, Wardha 442 001, India

[b]Department of Physics, Sant Gadge Baba Amravati University, Amravati 444 602, India

Received 9 March 2017; accepted 26 December 2017

PPy-Bi_2O_3-MOX (MOX=ZrO_2, Ag_2O and TiO_2) nanocomposites have been synthesized by *ex situ* approach. PPy-Bi_2O_3-MOX (MOX=ZrO_2, Ag_2O and TiO_2) nanocomposites sensors have been fabricated for LPG sensing application. The nanocomposites have been characterized by using X-ray diffraction (XRD), scanning electron microscopy (SEM), ultra violet visible spectroscopy (UV-Vis) and thermo gravimetric-differential thermal analyzer (TG-DTA) techniques. SEM micrograph exhibits irregular morphology, appropriate for gas sensing application. XRD reveals that all nanocomposites have amorphous nature. Among all the nanocomposites PBZr (PPy-Bi_2O_3-ZrO_2) nanocomposite sensor has found good LPG sensing performance. PBZr nanocomposite sensor also exhibits better selectivity and stability against LPG. This sensor has low operating temperature against LPG of the order of 323 K and fast response and recovery time.

Keywords: Polypyrrole, Film deposition, Gas sensors, LPG sensing

1 Introduction

Rising demands of sensing devices have attracted the attention of researchers across the globe toward efficient gas sensing materials[1]. Nanotechnology is the key solution, with the help of which it is possible to produce efficient sensing materials by altering shape and size. From last two decades, inorganic material remains important class for gas sensing application but to resolve the shortcomings of inorganic material based sensor, organic materials play important role[2,3]. In these organic materials, polypyrrole (PPy) has very interesting physical and chemical properties, appropriate for gas sensing application[4,5]. This may be due to its good electrical properties and sensitive nature towards the target gas based sensor is that the electrical properties spoil due to atmospheric changes. This results show poor stability. Therefore, addition of metal oxide in PPy matrix is the effective solution. In the present work, we studied the LPG sensing properties of PPy-Bi_2O_3-MOX (MOX=ZrO_2, Ag_2O and TiO_2) nanocomposites. Some reports in literature shows that PPy is potent candidate for gas sensing application. Carquigny *et al.* have prepared PPy thin films by electrochemical processing as sensitive layer for the micro-gas-sensing application. This study shows that temperature has great influence on electrical response of the sensors. Experimentation of this work demonstrated that as-prepared thin film of PPy has good ammonia sensing characteristics at room temperature[6]. Rawal *et al.* have tested the ammonia gas sensing characteristics of PPy nanowires which are synthesized by chemical route. This study also proves that the morphology has great impact on sensing characteristics. The PPy nanowires (~6%) have higher sensing response than PPy nanoparticles[7] (~4%). Li *et al.* have prepared PPy nanoparticles by novel approach, using Triton X-100 micelles via soft template approach. As-prepared PPy particles have linear response towards acetone in concentrations larly, the prepared PPy particles have rapid response and recovery time is 9 s and 8.3 s, respectively[8]. Zou *et al.* have prepared Pd–TiO_2@PPy-based sensor for H_2 sensing application. This material system shows the sensitivity of 8.1% toward 1 vol% of H_2 gas, which is much greater than separate TiO2@PPy and PPy nanofibers. Pd– TiO_2@PPy composite has excellent reproducibility, stability and selectivity for H_2 gas[9]. Hong *et al.* have prepared the PPy- palladium nanocomposite for ammonia gas sensing application. Nanocomposite shows good response and recovery times of the order of 14 s and 148 s for 1000 ppm,

*Corresponding author (E-mail: sandeepwaghuley@sgbau.ac.in)

respectively. The gas sensing properties of nanocomposite shows direct dependence on the size of Pd nanoparticles and the morphology of the composite film[10]. Babaei *et al.* have synthesized nanostructure conductive PPy by constant current electrodeposition on interdigital electrodes for methanol sensing. This study demonstrated that PPy can be used to detect residual methanol content in the biodiesel samples[11].

In this work we synthesized *ex situ* PPy-Bi_2O_3-MOX (MOX=ZrO_2, Ag_2O and TiO_2) nanocomposites for LPG sensing application. The prepared nanocomposites have considerable low operating temperature value (323 K). The fabricated sensors have rapid response and recovery time.

2 Experimental Details

2.1 Materials

In the present work, monomer Pyrrole (AR grade) and oxidant ammonium persulphate (AR grade) SD fine, India was used as starting chemicals. The procured chemicals were used without any purification.

2.2 Sensor films preparation and experimental procedure

The *ex situ* approach was adopted for the preparation of PPy-Bi_2O_3-MOX (MOX=ZrO_2, Ag_2O and TiO_2) nanocomposites. For the preparation of nanocomposite, PPy-Bi_2O_3 matrix was prepared by loading 25 wt.% of Bi_2O_3 nanoparticles in PPy. Further, PPy-Bi_2O_3 matrix decorated with 5 wt.% of MOX (MOX=ZrO_2, Ag_2O and TiO_2). During *ex situ* process, acetone was used as organic media to prepare homogeneous mixture of constituents of nanocomposites. In this way, three different nanocomposites were prepared namely, PBZr (PPy-Bi_2O_3-ZrO_2), PBAg (PPy-Bi_2O_3-Ag_2O) and PBTi (PPy-Bi_2O_3-TiO_2). The prepared nanocomposites were washed several times to remove impurity and allow drying in hot air oven for 24 h. For gas sensing application, sensors were designed in chemiresistive form. The chemiresistors were fabricated by using screen printing method on glass substrate. The silver paint was used as ohmic electrode on both sides of chemiresistor. To check gas sensing response, chemiresistors were loaded in gas sensor assembly of specifications mentioned in our previous report[12].

2.3 Characterization techniques

The nanocomposite samples were characterized by X-ray diffractometer (XRD) on Rigaku Miniflex-II, X-ray diffractometer to check structure related aspects. The morphology of nanocomposites was investigated by using scanning electron microscope (SEM) on SEM-JEOL JSM-7500F. The thermal study of ex-situ nanocomposites were investigated through thermo gravimetric-differential thermal analysis (TG-DTA) on Shimadzu DTG-60h. The composition and structure of the nanocomposites investigated using Raman spectroscopy on Bruker RFS 27. The optical properties of samples recorded on Agilent Cary 60 spectrophotometer.

3 Results and Discussion

3.1 X-ray Diffraction and Scanning electron microscopy analysis

Figure 1(a-c) depicts the XRD pattern of ex-situ PBZr, PBAg, PBTi nanocomposites and arrow represents SEM micrographs of respective materials. XRD data shows that all nanocomposites samples have amorphous nature. The XRD results obtained for PBZr, PBAg and PBTi supported by Dubal *et al.*[13] and Palaniappan *et al.*[14]. The XRD pattern of all nanocomposites shows that two broad humps appear on peaks. It may be attributed to *ex situ* addition of constituents of nanocomposites. The micrographs of PBZr, PBAg and PBTi are shown in Fig. 1(a-c) have strongly agglomerated nature. The SEM micrographs show that nanocomposites have irregular morphology and particle size.

The Debye Scherer's formula is used to investigate the particle size of all three nanocomposites:

$$D = (K\lambda / \beta\cos\theta) \quad \ldots (1)$$

where D is average crystallite size (nm), K is a shapes factor (K=0.9), λ is the wavelength of X-ray source equals 1.540 Å, β is the full width at half maxima, and θ is the diffraction peak angle. The particle size of all three nanocomposites samples is listed in Table 1.

3.2 Raman spectroscopy

The Raman spectra of PBZr nanocomposite is shown in Fig. 2(a) and it comprises band at 1562 cm^{-1} assigned to the intercycle carbon–carbon stretching vibration. The oxidized region in composite is appeared through band at 1641 cm^{-1}. Similarly, oxidized region in PBAg due to Bi_2O_3 and Ag_2O seen at 921 and 1061 cm^{-1} in Fig. 2(b). The Fig. 2(c) shows the PBTi nanocomposite comprises peak of oxidized region[15,16] around 1635 cm^{-1}. The UV-Vis spectra of PBZr, PBAg and PBTi are presented in Fig. 2(d). The PBZr, PBAg and PBTi nanocompsoites shows intense absorption tail around 228 nm, which is

attributed to metal oxide nanoparticles present in polymeric matrix. Nearly flat region appears in all samples between 325-500 nm is assigned to the surface plasmon resonance band overlapped with absorption band[17] of PPy.

3.3 Thermogravimetric-differential thermal analysis

Figure 3(a-c) depicts the TG-DTA curves of PBZr, PBAg and PBTi, respectively. The % weight loss curve shows common observable deep (endothermic peak) in the range 344-352 K, assigned to continuous mass loss due to removal of residual solvent and constituted water remaining in the nanocomposite. Many researchers also attribute the weight loss due to removal of constituted water. All nanocomposites show two apparent mass losses peaks on % weight loss curve. Similarly mass loss curve shows endothermic peaks in the range 532-546 K in all nanocomposites attributed to degradation of organic matter and breakdown of polymeric network[18]. Thermal stability for gas sensing application is key parameter. All nanocomposites were almost thermally stable below 400 K.

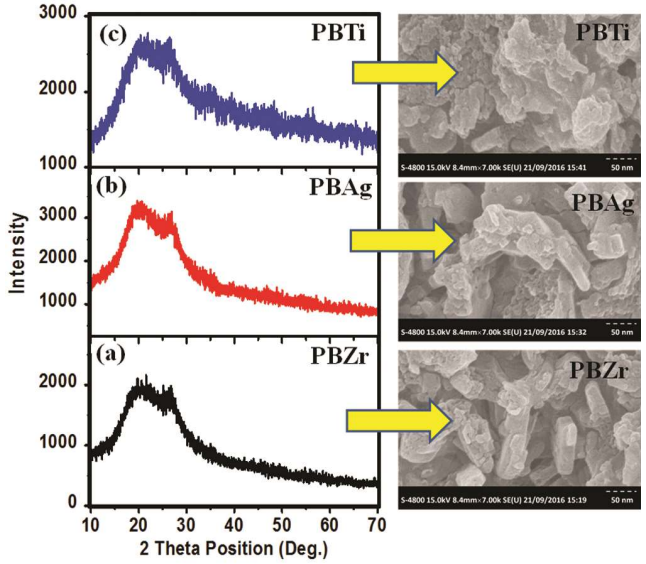

Fig. 1 – XRD pattern and respective SEM images of *ex situ* (a) PBZr, (b) PBAg and (c) PBTi.

3.4 Gas sensing properties

In our study, first selectivity nature of all nanocomposites is investigated. Figure 4(a) shows selectivity response of PBZr, PBAg and PBTi nanocomposite samples checked towards CO_2 and LPG for 500 ppm at room temperature (303 K). This study shows that all nanocomposites are more selective towards LPG than CO_2 gas. It indicates that our nanocomposite materials are more selective towards reducing gas. Gas sensing response of PBZ, PBA and PBT nanocomposite as a function of LPG concentration is shown in Fig. 4(b). The PBZr shows

Table 1 – The particle size of PBZr, PBAg and PBTi nanocomposite samples.

Sample	Peak position of amorphous halo (θ) (°)	Particle size (nm)
PBZr	11.44	16.253
PBAg	10.03	16.178
PBTi	10.28	16.190

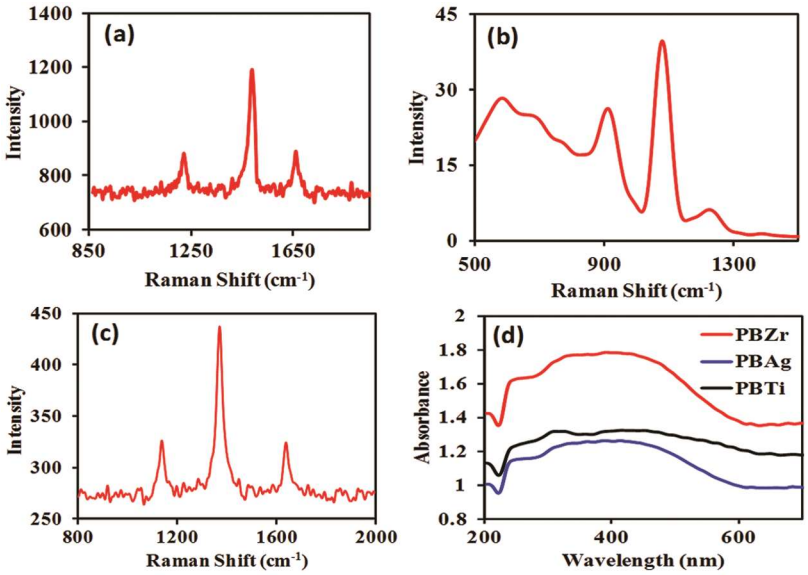

Fig. 2 – Raman spectrum of *ex-situ* (a) PBZr, (b) PBAg, (c) PBTi and (d) UV-Vis spectrum of PBZr, PBAg and PBTi.

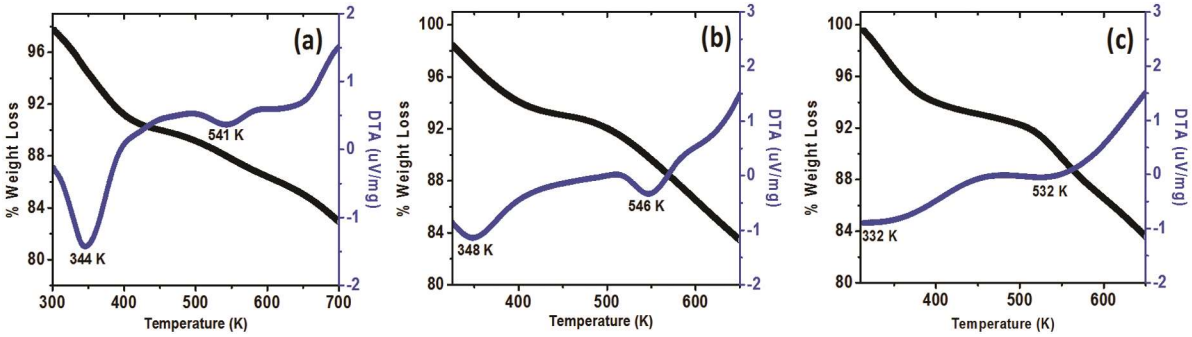

Fig. 3 – TG-DTA of *ex situ* (a) PBZr, (b) PBAg and (c) PBTi.

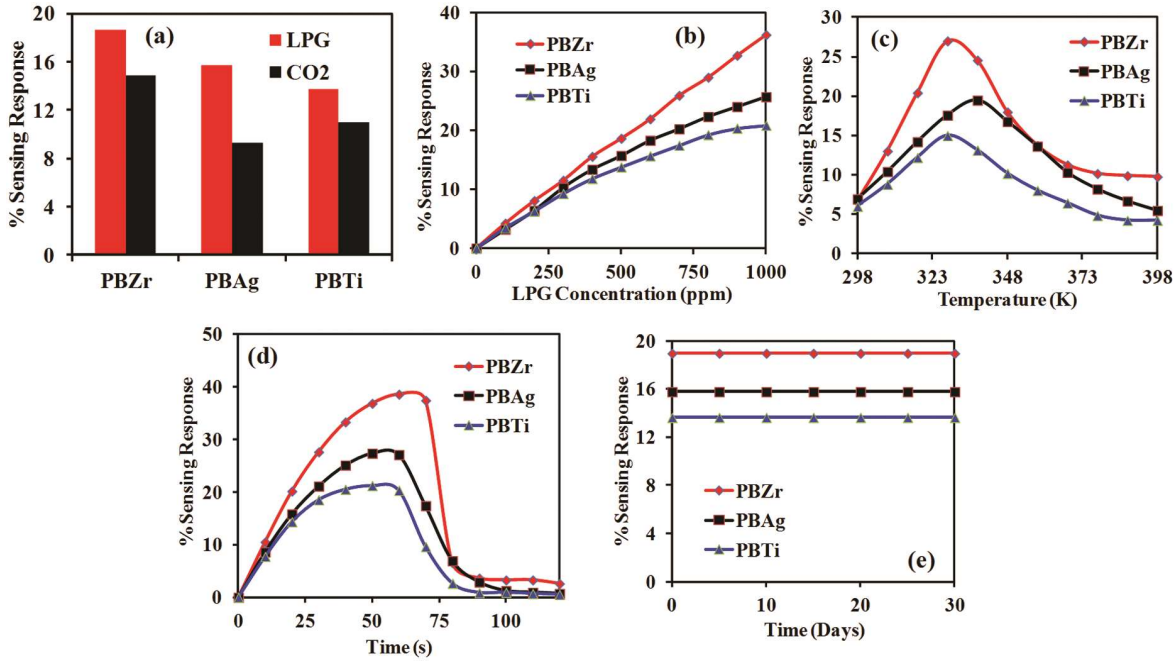

Figure 4 – (a) Selectivity, (b) gas sensing, (c) operating temperature, (d) transient and (e) stability response of PBZr, PBAg and PBTi nanocomposites.

highest LPG sensing response among all nanocomposites. Sensing response curve of PBZr shows almost linear behavior up to 1000 ppm at room temperature. In case of LPG sensing, the operating temperature characteristics play crucial role, as LPG is highly inflammable gas. In our study all nanocomposites Fig. 4(c) have found operating temperature around 323 K, which is much below the auto-ignition temperature of LPG. Figure 4(d) shows the response and recovery response of PBZr, PBAg and PBTi checked towards the 500 ppm LPG. All nanocomposites have rapid response as well as recovery values. The recovery time is greater than response time, it may be due to gas molecules diffused with sensing surface and it takes time for dissociation process. Figure 4(d) shows the transient response of PBZ, PBA and PBT nanocomposites towards 500 ppm LPG to check response and recovery time. From figure it is observed that all nanocomposite samples have rapid response towards the LPG gas. All nanocomposites achieved highest sensing response value in 50 s and recovery to their original value in 70 s. Stability response is very important aspect of any sensor in order to reproduce results. Figure 4(e) shows the stability response of *ex situ* PBZr, PBAg and PBTi nanocomposites for 500 ppm LPG at room temperature (303 K). Plot clearly shows that all nanocomposites have almost stable response for 30 days against LPG and atmospheric changes.

4 Conclusions

We have successfully prepared *ex-situ* PPy-Bi_2O_3-MOX (MOX=ZrO_2, Ag_2O and TiO_2) nanocomposites. The PPy-Bi_2O_3-MOX nanocomposite sensors

fabricated by screen printing technique are employed for LPG sensing application. The physico-chemical characterizations reflected the structure and morphology suitable for gas sensing application. The selectivity response shows that as-prepared nanocomposites have more selective nature towards LPG than CO_2 gas. Among these nanocomposites, PPy-Bi_2O_3-ZrO_2 (PBZr) have found optimized LPG sensing properties such selectivity, sensing response and stability. The operating temperature for PBZr sensor was found to be 323 K which is main accomplishment of present work due to temperature 323 K that is much below auto-ignition temperature of LPG.

Acknowledgement

Authors are very much thankful to the Head, Department of Physics, Sant Gadge Baba Amravati University, Amravati, India for providing necessary facilities.

References

1 Kwon O S, Hong J Y, Park S J, Jang Y & Jang J, *J Phys Chem*, 114 (2010) 18874.
2 Bai H & Shi G, *Sensors*, 7 (2007) 267.
3 Liu H, Kameoka J, Czaplewski D A & Craighead H G, *Nano Lett*, 4 (2004) 671.
4 Yoon H, Chang M & Jang J, *J Phys Chem*, B 110 (2006) 14074.
5 Lü Q, *Microchim Acta*, 168 (2010) 205.
6 Carquigny S, Sanchez J, Berger F, Lakard B & Lallemand F, *Talanta*, 78 (2009) 199.
7 Rawal I & Kaur A, *Sens Actuators*, 203 (2013) 92.
8 Fake L, Hang L, Hongmin J, Kejun Z, Kai C, Shuangrong J, Wenbin J, Ya Shanga W L, Shaoli D & Ming C, *Appl Surface Sci*, 280 (2013) 212.
9 Yongjin Z, Qingyong W, Dadi J, Cuili X, Hailiang C, Shujun Q, Huanzhi Z, Fen X, Lixian S & Shusheng L, *Ceram Int*, 42 (2016) 8257.
10 Lijie H, Yang L & Mujie Y, *Sens Actuators*, 145 (2010) 25.
11 Mohsen B & Naader A, *Sens Actuators*, 183 (2013) 617.
12 Nemade K R & Waghuley S A, *J Electron Mater*, 42 (2013) 2857.
13 Dubal D P, Patil S V, Jagadale A D & Lokhande C D, *J Alloys Comp*, 509 (2011) 8183.
14 Palaniappan S P & Manisankar P, *Mater Chem Phys*, 122 (2010) 15.
15 Le H N T, Bernard M C, Garcia-Renaud B & Deslouis C, *Syn Metals*, 140 (2004) 287.
16 Faulques E, Wallnoefer W & Kuzmany H, *J Chem Phys*, 90 (12) (1989) 7585.
17 Kate K H, Singh K & Khanna P K, *Nano-Metal Chem*, 41 (2011) 199.
18 Khorami H A, Keyanpour-Rad M, Eghbali A & Vaezi M R, *J Nanostruct*, 2 (2013) 427.